Au/ZrO$_2$ catalysts for LT-WGSR: Active role of sulfates during gold deposition

Maela Manzoli [a], Flora Boccuzzi [a,*], Valentina Trevisan [b,c], Federica Menegazzo [b,c], Michela Signoretto [b,c,**], Francesco Pinna [b,c]

[a] Department of Chemistry, IFM and NIS Centre of Excellence, University of Torino, Italy
[b] Department of Chemistry, Cà Foscari University, Calle Larga S.Marta, Dorsoduro 2137, 30123 Venezia, Italy
[c] INSTM-UdR Venezia, Italy

ARTICLE INFO

ABSTRACT

The effect of the addition of various amounts of sulfates to a zirconia support and its possible role during the Au deposition–precipitation step was examined. The high activity showed by the Au/ZrO$_2$ catalysts in the WGS reaction was enhanced by the action of sulfates on the support. SO$_4^{2-}$ addition to zirconia brings a higher gold dispersion due to (i) the larger surface area and (ii) the positive role of SO$_4^{2-}$ groups that determine the deposition of Au in the form of highly dispersed non-metallic gold clusters in close contact with the support.

© 2010 Elsevier B.V. All rights reserved.

1. Introduction

Catalysis by gold nanoparticles is a topic of current interest, as proved by the exponential growth of the papers on this subject [1]. In fact gold supported on oxides or carbon, once considered catalytically inert, is now firmly established as an effective catalyst. The catalogue of reactions that it can catalyze is really wide. In particular, supported gold particles are effective catalysts for low-temperature CO oxidation, selective oxidation of propene to propene oxide, water-gas shift reaction, NO reduction, selective hydrogenation of acetylene (or butadiene) [2].

The relationship between activity, microstructure and nature of the catalytically active gold sites is, up to now, not fully understood. There is still a big debate on the role played by the preparation method and by the acidity of the support and its modification with surface species like sulfates on the nature of the resulting gold species. Experimental data on selective oxidation [3] indicate that there is a limiting diameter size (1.5–2 nm) that discriminates between active samples from the inactive ones. This is the same limiting size observed for both "active" and "inactive" supports, as BN, SiO$_2$ and C on which Au is dispersed. It appears

related to an intrinsic modification of the electronic structure of non-metallic gold nanoclusters with respect to the metallic nanoparticles. As for the water-gas shift reaction, cationic gold or highly dispersed non-metallic gold clusters in close contact with the support are usually considered active sites [4]. Very recently, an unprecedented reactivity in the HCOOH decomposition into H$_2$ and CO$_2$ of Au-based catalysts for fuel cells designed for portable use has been reported [5]. It has been shown that the reactivity derives from highly dispersed and stable Au species, undetectable by transmission electron microscopy. The primary role of the support is to have a high concentration of nucleation sites for gold and to avoid coalescence and agglomeration. Characteristics such as surface area, presence of surface hydroxyl groups, density of defects, modification of the surface acidity and of the predominant crystalline phase can influence its adsorption ability [1]. We have recently focused our attention on gold based catalysts supported on zirconia [6,7]. The choice of zirconia as support is due to its intrinsic chemical and physical characteristics that can be adjusted by choosing different precursors and synthesis conditions. Moreover, the addition of dopants, in particular sulfates, increases surface acidity, retards crystallization and enhances the surface area [8]. ZrO$_2$ has also been found to be a very suitable support for gold [9–11]. We have optimised a method for dosing low coordination sites exposed at the surface of gold supported on different oxides [12]. This procedure is based on the combined use of pulsed CO chemisorption measurements and FTIR spectroscopy of adsorbed CO, both techniques being applied in well controlled experimental conditions. It has been shown that the amount of low

* Corresponding author. Tel.: +39 0116707542; fax: +39 0116707855.
** Corresponding author at: Department of Inorganic, Physical and Materials Chemistry and NIS Centre of Excellence, Università di Torino, Via Pietro Giuria 7, 10125 Torino, Italy. Tel.: +39 041 2348650; fax: +39 041 2348517.
E-mail addresses: flora.boccuzzi@unito.it (F. Boccuzzi), miky@unive.it (M. Signoretto).

coordinated gold sites exposed at the surface of some Au/ZrO$_2$ systems [7] is up to 10 times higher than the one observed for standard Au/TiO$_2$ by WGC (World Gold Council). In fact, a very good relationship between catalytic activity and chemisorption data has been evidenced [13], indicating that the chemisorption test is suitable for a preliminary evaluation of the Au/ZrO$_2$ systems used for the LT-WGSR. We have recently demonstrated [13] that gold supported on sulfated zirconia is more active than the samples on plain zirconia in the LT-WGSR. This higher activity is probably due to a larger surface area of sulfated zirconia that leads to a better dispersion of gold on the surface. It would be very interesting to clarify the role of SO$_4^{2-}$ in the delicate phase of gold deposition on the support and subsequently on dispersion and catalytic activity. The goal of the present work is to examine the effects of the addition of various amounts of sulfates to a zirconia support and to check their role during the Au deposition–precipitation step.

2. Experimental

2.1. Catalyst preparation

Zirconia was prepared by a two-step synthesis technique. Zr(OH)$_4$ was prepared by precipitation from ZrOCl$_2$·8H$_2$O at constant pH (pH = 8.6) and then aged under reflux conditions for 20 h at 363 K, washed free from chloride (AgNO$_3$ test) and dried at 383 K overnight. The hydroxide was then sulfated with (NH$_4$)$_2$SO$_4$ (Merck) by incipient wetness impregnation in order to obtain a 1, 2, 4, 8 wt% amount of sulfates respectively on the final support. Sulfated zirconium hydroxides were then calcined in air (30 mL/min STP) by slowly heating from room temperature to 923 K over 7 h, and keeping this temperature for 6 h. The different SO$_4^{2-}$ amount is defined in the denomination of the supports: ZS1, ZS2, ZS4 and ZS8 respectively. 1 wt% of gold was added by deposition–precipitation (dp) at pH = 8.6: the oxide support was suspended in an aqueous solution of HAuCl$_4$·3H$_2$O for 3 h and the pH was controlled by the addition of NaOH (0.5 M).

Moreover, a sample was synthesized by dp after the sulfates removal from the zirconia. A complete extraction of sulfates was obtained, as previously reported [14], by suspending the calcined support in an aqueous solution of NaOH (0.5 M) at pH = 8.6. Then gold was deposited by dp as previously reported (inverted sample denoted with the initial letter I). After filtrations all samples were dried at 308 K overnight and part of the catalysts were finally calcined in air for 1 h by slowly heating (60 K/h) from 298 to 453 K.

2.2. Methods

Surface area and pore size distributions were obtained from N$_2$ adsorption/desorption isotherm at 77 K, using a Micromeritics ASAP 2000 Analyser. Sulfated zirconia supports (400 mg) were pre-treated at 570 K for 2 h under vacuum, while the final catalysts (300 mg) were pre-treated at room temperature for 6 h under vacuum. Surface area was calculated from the N$_2$ adsorption isotherm by the BET equation [15] and pore size distribution was determined by the BJH method also applied on the adsorption branch [16]. Total pore volume was taken at p/p_0 = 0.99.

The sulfate content of all samples was determined by ion chromatography (IC) [14]. Sulfate concentration was calculated as the average of two independent analyses, each including two chromatographic determinations.

The gold amount was determined by atomic adsorption spectroscopy after microwave disgregation of the samples (100 mg).

X-ray powder diffraction (XRD) patterns were measured by a Bruker D8 Advance diffractometer equipped with a Si(Li) solid state detector (SOL-X) and a sealed tube providing Cu K$_\alpha$ radiation. Measuring conditions were 40 kV × 40 mA. Apertures of divergence, receiving and detector slits were 1°, 1°, and 0.3° respectively. Data scans were performed in the 2θ ranges 15–55° and 35–40° with 0.02° step size and counting times of 3 s/step and 10 s/step respectively.

CO pulse chemisorption measurements were performed at 157 K in a lab-made equipment. Before the analysis the following pretreatment was applied: the sample (200 mg) was reduced in a H$_2$ flow (40 mL/min) at 423 K for 60 min, cooled in H$_2$ to room temperature, purged in He flow and finally hydrated at room temperature. The hydration treatment was performed by contacting the sample with a He flow (10 mL/min) saturated with a proper amount of water. The sample was then cooled in He flow to the temperature chosen for CO chemisorption (157 K) [7].

Thermal analyses (TG/DTA) were performed on a NETZSCH STA 409 PC/PG instrument in flowing air (20 mL/min) with temperature rate set at 5 K/min in the 300–1300 K temperature range.

TPO measurements were carried out to determine the substances released during the TG/DTA thermal treatment, in a lab-made equipment: samples (100 mg) were heated with a temperature rate of 10 K/min from 300 to 1300 K in air (40 mL/min). The effluent gases were analyzed by a Genesys 422 quadrupole mass analyzer (QMS). The signals for masses 18, 28, 44, 48, 64 were recorded.

FTIR spectra were taken on a Perkin-Elmer 1760 spectrometer (equipped with a MCT detector) with the samples in self-supporting pellets introduced in a cell allowing thermal treatments in controlled atmospheres and spectrum scanning at controlled temperatures (from 120 to 300 K). From each spectrum, the spectrum of the sample before the inlet of CO was subtracted. Band integration and curve fitting have been carried out by Spectra Calc (Galactic Industries Co.). The spectra were normalised with respect to the gold content of each pellet. The pretreatment of the samples was: (i) reduction in H$_2$ at 423 K; (ii) outgassing H$_2$ to room temperature (r.t.); (iii) hydration at r.t.; (iv) outgassing water at r.t. to obtain the same residual pressure (2.5 × 10^{-2} mbar H$_2$O).

2.3. Catalytic activity measurement

WGSR was performed in a fixed-bed flow reactor at atmospheric pressure and in a temperature range from 423 to 453 K. The following conditions were applied: space velocity = 9400 h^{-1}; catalyst volume = 0.5 cm^3 (35–50 mesh) diluted to 1.5 cm^3 with quartz sand (Carlo Erba; 35–50 mesh); gold supported samples were previously subjected to a slow (60 K/h) thermal activation in air (50 mL/min) from room temperature to 453 K, kept at this temperature for 1 h in the same air flow and then cooled in N$_2$

Table 1
Surface features and SO$_4^{2-}$ amounts of the supports.

Sample	Nominal SO$_4^{2-}$ (wt%)	Found SO$_4^{2-}$ (wt%)	Surface area (m^2/g)	Pore diameter (nm)	SO$_4^{2-}$ (groups/nm^2)
ZS1	1	1.0	79	10.9	0.79
ZS2	2	2.0	99	8.7	1.27
ZS4	4	3.6	115	7.0	1.96
ZS8	8	4.0	119	6.7	2.11

(50 mL/min). Then the catalysts were heated again (180 K/h) in a 2% hydrogen/nitrogen mixture (50 mL/min) up to 453 K; once this temperature was reached, the gas feed composition was slowly changed to pure hydrogen (50 mL/min) and after 1 h changed to the feed mixture: 1.9% vol. CO, 39.7% vol. H_2, 9.5% vol. CO_2, 11.4% vol. N_2, 37.5% vol. H_2O [6,13]. The progress of the reaction was followed by gas-chromatographic analysis of the converted mixture at the reactor outlet (packed column Carbosphere, TCD detector, V loop = 1 mL).

3. Results and discussion

3.1. Catalysts characterization

Sulfated zirconia supports and gold samples were analyzed by ion exchange chromatography to determine the amount of sulfate groups and the results are reported in Table 1. As it can be seen, tests of sulfates carried out on the sulfated zirconium hydroxides calcined at 923 K show that the SO_4^{2-} wt% found is much lower than the expected value. In particular, the difference between the nominal and the actual value increases with the rise of the amount of anions on the support. It is already known [17] that the elimination of sulfates occurs during the calcination step and that the SO_4^{2-} amount that remains at the end of this process is strictly connected with the calcination conditions. This sulfates content is related to the amount of anions that are more firmly bound to Zr^{4+} groups, i.e. anchored to Zr^{4+} groups not placed in the corners of ZrO_2 crystals. Such cations are in fact highly energetic sites (i.e. highly uncoordinated). The groups that are situated over them are more easily eliminated from the oxide surface during the calcination step. In other words, there is a sort of selective elimination of sulfates from highly energetic crystallographic defects [18]. Therefore the relationship between sulfates loss and their amount depends on the maximum value of anions that the oxide can keep under the calcination conditions. For the samples examined in the present work we can assume a maximum of about 4% (wt/wt).

Such behavior can be noted in the thermal DTG/DTA analyses that were carried out on the four uncalcined supports in order to observe their behavior during calcination and that are reported in Fig. 1. From the DTG curves it is evident that all the samples show a significant weight loss between 300 and 400 K, in correspondence to large endothermic peaks in the DTA curve, due to the release of water from the surface of the catalysts. Besides, at about 470 K the DTG and DTA profiles show another weight loss due to zirconium hydroxide dehydroxylation [19]. Above 900 K the ZS8 support shows a sharp peak of weight loss up to 1000 K, in correspondence to an endothermic peak in the DTA curve, which is related to sulfate decomposition. Similarly, the DTG spectra of ZS4 support
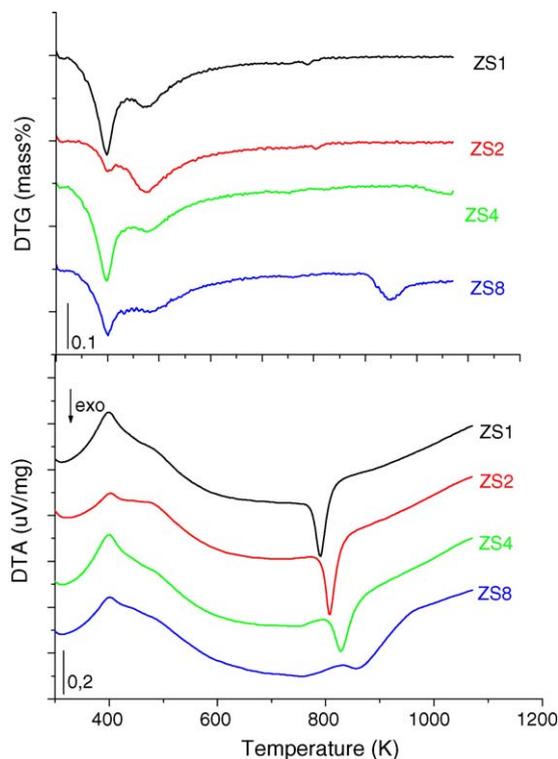

Fig. 1. DTA and DTG curves for the supports.

show a broad peak of weight loss at slightly higher temperatures (1000 K). On the contrary, in the ZS1 and ZS2 profiles no significant weight loss was observed above 600 K, probably because the mass decrease was under the detection limits. In the 750–900 K region the DTA profiles of the four supports show sharp exothermic peaks occurring without weight loss; this can be associated to zirconia phase transition (from amorphous to crystalline) [20–22]. It is interesting to notice that with the increase of the SO_4^{2-} loading there is a progressive shift of the peak from 800 K (ZS1) to 870 K (ZS8) and a corresponding decrease of its intensity. This result clearly shows that the effect of sulfates on zirconium oxide is to shift the crystallization processes towards higher temperatures during calcination treatment [23]. A further confirmation of this result comes from the physisorption analyses that are reported in Table 1. The physisorption isotherms and pore diameter distributions are very similar to the ones reported in Fig. 2 for the samples containing 1 wt% of gold, and are therefore not shown for the sake of simplicity. All samples show type IV isotherms with a hysteresis loop typical of mesoporous materials. Higher SO_4^{2-} loaded
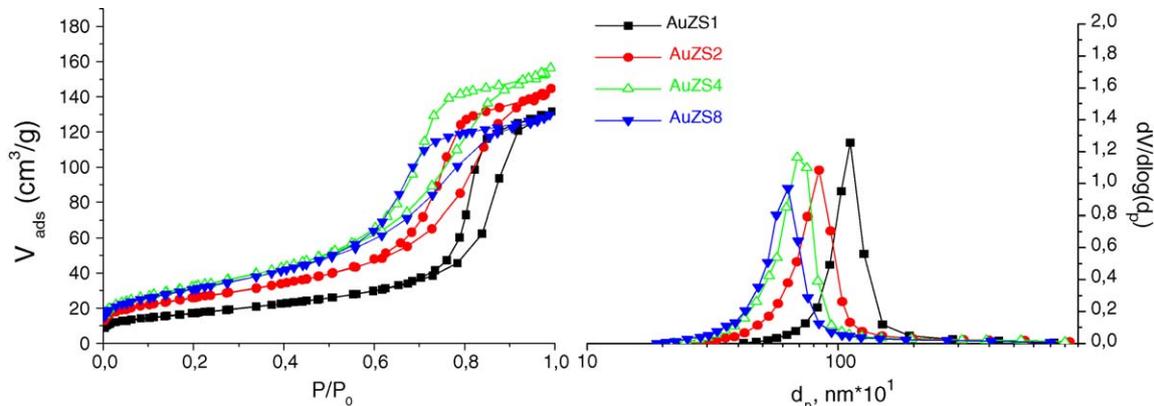

Fig. 2. N_2 physisorption isotherms and BJH pore size distributions of catalysts.

Table 2
Characterization and activity data of the samples.

Sample	Au found (wt%)	Surface area (m^2/g)	Pore diameter (nm)	mlCO$_{(273 K)}$/gAu	molCO/molAu	Conversion at 453 K (%)
AuZS1	0.74	73	11.1	30.8	0.271	76
AuZS2	0.79	93	8.0	37.2	0.327	83
AuZS4	0.83	111	6.6	41.7	0.366	83
AuZS8	0.86	112	6.0	40.9	0.359	83

catalysts show higher specific surface area values than the less sulfated ones, ranging from 73 (AuZS1) to 112 m^2/g (AuZS8). It is very interesting to note the progressive shift of the pore size distribution curves towards smaller diameters with the increasing of the doping anion content. Such reduction of mean pore size is significant since it achieves almost 50%. A comparison between Tables 1 and 2 points out that surface area and porosity are very similar for the supports and the corresponding catalysts and that they are not modified by the gold dp technique. In conclusion, we can remark that the effect of sulfates on zirconium oxide is to increase its surface area and reduce the mean pore size, shifting crystallization processes towards higher temperatures during calcination treatment.

Table 2 shows the gold content of the catalysts, while the sulfates amount in the final samples are not reported because no sulfates are present in the final catalysts as previously verified [6,13]. This is not unexpected, as the detachment of sulfate groups occurs during the dp as a consequence of the basic conditions.

X-ray diffraction patterns for the gold based samples in the range of 2θ between 20° and 50° are reported in Fig. 3. No significant difference is observed in the crystallinity of the fours samples. It is known [24] that the hydroxides sulfation promotes the formation of the tetragonal phase of zirconia (t-ZrO$_2$) with respect to the monocline one (m-ZrO$_2$). XRD analyses confirm such trend and this is particularly true for the AuZS1 sample. In addition no peak related to the presence of gold crystallites is observable, suggesting a high dispersion of gold particles on the support surface. Such very high Au dispersion is confirmed by the results of CO chemisorption analyses. In fact we have recently demonstrated that CO chemisorption performed by a pulse flow system at 157 K on suitably pre-treated samples can be taken as a method for the quantitative determination of the gold sites on Au/ZrO$_2$ catalysts [7]. Moreover we have recently verified [13] the close connection between chemisorption data and catalytic results in the LT-WGSR, pointing out that Au dispersion in zirconia catalysts is a very

important parameter for their preliminary evaluation. Results of pulse flow CO chemisorption measurements for the catalysts object of the present work are reported in Table 2. The molar ratio between CO and Au is very similar for the AuZS2, AuZS4 and AuZS8 samples, indicating the same dispersion for these catalysts. The values are very high [7] and we can determine a very small gold particle size. On the contrary, the AuZS1 sample shows the lowest molCO/molAu ratio, meaning gold particles with dimensions larger than the other samples. This is probably due to the lower surface area of the ZS1 support.

3.2. Activity data

The effect of the SO$_4^{2-}$ addition on the support and its consequences on the activity in the low-temperature water-gas shift reaction has been investigated. In Table 2 the conversions obtained with the 1 wt% gold-loaded catalysts on the four supports are reported. The sample containing less sulfates (AuZS1), which is the one with the lowest surface area and dispersion, shows also the lowest catalytic activity. On the contrary, conversions obtained for the AuZS2, AuZS4 and AuZS8 samples are noticeably higher and very much alike. We are able to define an ideal range for the sulfates concentration. The addition of small SO$_4^{2-}$ amounts on the support is not enough, while the charging of zirconium hydroxide with 2–8% of sulfates allows an improvement of the dispersion of gold nanoparticles and of the catalytic performance.

3.3. Investigation on the effects of sulfates

We have previously discussed the positive role of sulfates that alter the structural properties of the support enhancing its specific surface area and thus favouring a better dispersion of gold particles. However, the final catalysts do not contain sulfates anymore, due to the methodology of gold deposition–precipitation that is carried out at a basic pH [6,7,13]. Sulfates do not behave as promoters of the gold active phase in the final samples, but they only act as structural promoters of the support. We have therefore synthesized a new gold catalyst after sulfates remotion from zirconia. In this way we can deposit gold over two different supports with an identical surface area, one containing sulfates and the other one SO$_4^{2-}$ free. Fig. 4 shows the main characteristics of the two different catalysts prepared on the ZS2 support: one synthesized by dp on the sulfated support (AuZS2), and the other one prepared after the removal of sulfates (IAuZS2). They have the same surface area and the same gold content, but differ a lot in dispersion and catalytic activity. In particular the sample prepared on a SO$_4^{2-}$ free support chemisorbs almost half the CO of the other one and has a lower WGS conversion. This is a clear indication that sulfates have an active role during the step of Au dp.

FTIR measurements after CO adsorption at 157 K on both AuZS2 and IAuZS2 samples were performed in order to elucidate the role of sulfates on the nature of gold sites in the final catalyst. The samples were reduced in H$_2$ at 423 K and hydrated at r.t. before CO chemisorption at 157 K, following the same procedure used for the quantitative chemisorption experiments. In Fig. 5 the amounts of CO chemisorbed vs. the integrated intensities of the FTIR CO bands, normalised to the gold content, are reported for AuZS2 (indicated
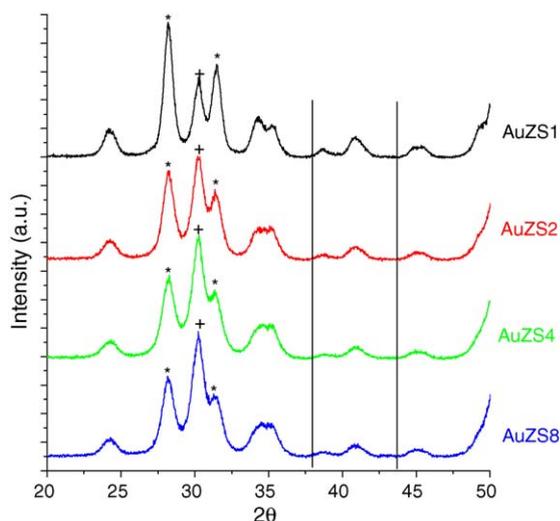

Fig. 3. XRD patterns of catalysts (★) monocline zirconia and tetragonal zirconia (+).
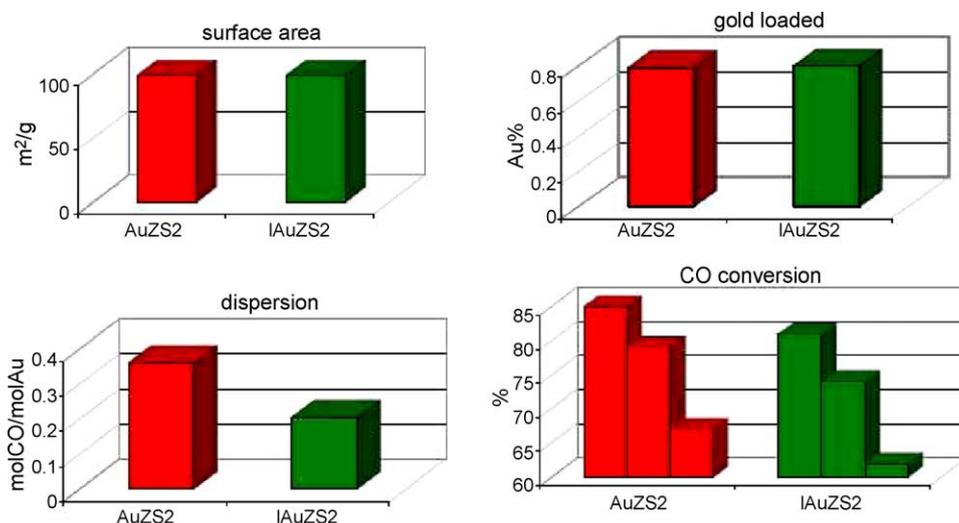
Fig. 4. Comparison between AuZS2 and IAuZS2 samples: surface area, gold content, chemisorption results and CO conversion.

by a triangle) and IAuZS2 (indicated by a circle). These results are plotted together with those previously reported [7] for a series of Au/ZrO$_2$ catalysts prepared by dp and with different gold loadings (square). In Ref. [8] a quite good linear relationship between the amounts of CO chemisorbed and the integrated peak intensities was found. The point related to AuZS2 (triangle) is also quite close to this straight line. Therefore, the largest fraction of gold adsorbing sites present on this sample has the same nature of the previously reported samples, i.e. highly dispersed neutral non-metallic gold clusters [7].

On the other hand, the IAuZS2 (circle) deviates strongly from the linearity. In fact, the integrated area of the CO band related to this sample is higher than the one related to AuZS2 and the calculated absorption coefficient raises to 2.9 cm^{-1} mol^{-1} × 10^4.

Moreover, the deviations from linearity observed for AuZS2 (small) and for IAuZS2 (large) and the differences in the absorption coefficients of these two samples in respect to the ones reported in Ref. [6], can be attributed to the co-presence of Au nanoparticles, as well as to the non-metallic gold clusters. The absorption coefficient associated to the CO on gold nanoparticles was previously obtained for Au/TiO$_2$ and Au/Fe$_2$O$_3$ [12]. In particular, the gold adsorbing sites exposed at the surface of the metal nanoparticles are
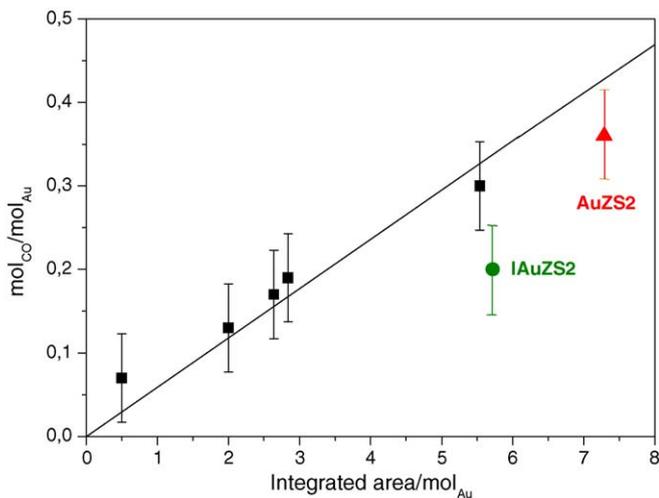

Fig. 5. CO chemisorbed amounts vs. integrated intensities of the FTIR CO bands normalised to the gold content for the AZS2 (triangle) and IAZS2 (circle) samples in comparison with a series of Au/ZrO$_2$ catalysts (square).

characterized by an absorption coefficient of the adsorbed CO that is 3.2 cm^{-1} mol^{-1} × 10^4 [12], this value being twice the one associated to the highly dispersed non-metallic clusters (1.5 cm^{-1} mol^{-1} × 10^4) [7]. Hence, the CO adsorbed on gold nanoparticles, having an absorption coefficient larger than the one related to the non-metallic gold clusters, can contribute significantly to the final integrated area of the FTIR CO band.

A deconvolution of the FTIR CO band has been performed, in particular two components have been identified in the case of the AuZS2 catalyst: one related to CO on well isolated gold adsorbing sites, i.e. highly dispersed non-metallic clusters, the other one related to gold sites exposed at the surface of the nanoparticles. The ratio between the gold adsorbing sites on the non-metallic clusters and those exposed at the surface of the nanoparticles was found to be 2.8. This value was obtained using the appropriate absorption coefficients for the two species, 1.5 and 3.2 cm^{-1} mol^{-1} × 10^4 respectively, as reported in the Refs. [7,12]. This result indicates that on the AuZS2 sample the amount of sites belonging to neutral non-metallic clusters is three times larger than the abundance of adsorbing sites of the nanoparticles. A different situation has been noticed for the IAuZS2 sample. In this case the calculated ratio between the sites related to the non-metallic clusters and the sites of the nanoparticles is only 1.55.

The FTIR spectra analysis suggests a possible additional explanation of the positive effect of sulfates: the production of larger amounts of small clusters, as shown in schemes reported in Fig. 6. The IAuZS2 catalyst, in which the sulfates were removed before gold dp, does not have preferential OH groups on the zirconia surface (see left panel of Fig. 6). For this sample we can assume a mechanism similar to the one reported for gold on titania catalysts by Moreau et al. [25]: at pH = 8.6 the Au (OH)$_3$ species are deposited everywhere on the negatively charged support, reacting with the already present surface OH groups. Also in the AuZS2 sample (right panel) the Au(OH)$_3$ species react with the OH groups of the zirconia surface. However, in this case the reacting OH sites are mainly produced by the removal of the sulfate groups, i.e. while the pH is raising. These "nascent" OH (colored in blue in the scheme) may react with the gold complexes in solution, forming quite isolated gold grafted species at the surface of AuZS2 and, after calcination, very small Au$_2$O$_3$ clusters. Consequently, the gold dispersion of this sample is higher than the one observed on the IASZ2 sample, where the sulfates were removed before introducing gold: the Au(OH)$_3$ dp occurs everywhere on the support and after calcination a larger amount of bigger nanoparticles is produced.
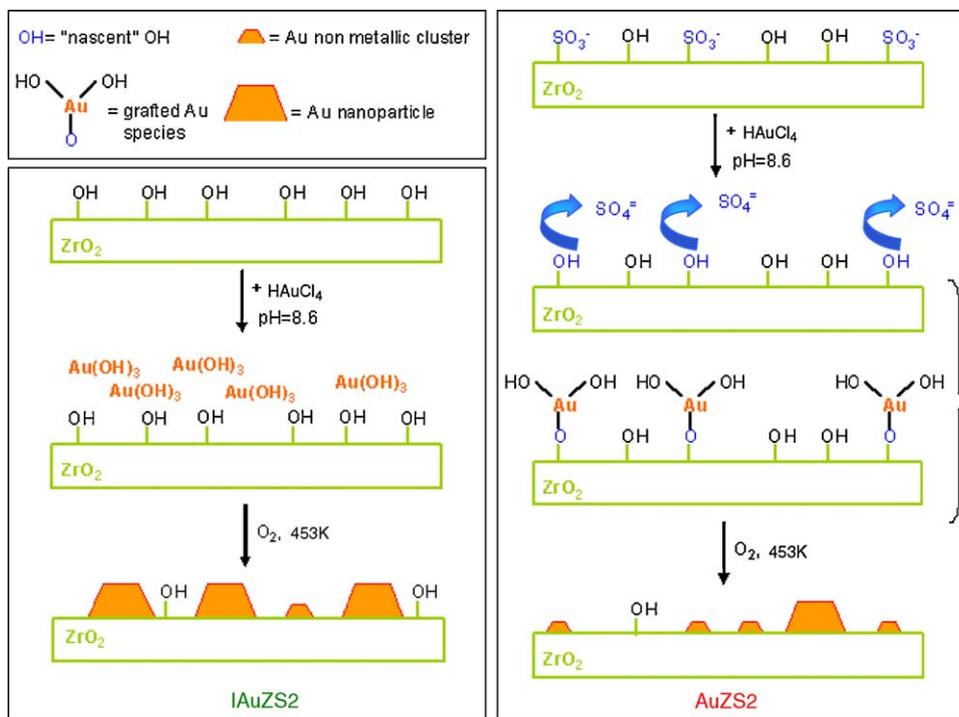
Fig. 6. Schematization of the deposition–precipitation (dp) process for the AuZS2 and IAuZS2 samples. (For interpretation of the references to color in this figure, the reader is referred to the web version of the article.)

4. Conclusions

The high activity showed by gold on zirconia catalysts in the water-gas shift reaction was enhanced by the action of sulfates on the support. Such SO_4^{2-} promotion is carried on in a well defined concentration range. We have demonstrated that sulfates addition to zirconia brings a twofold advantage: (i) a higher gold dispersion due to higher surface area and (ii) a higher gold dispersion due to the positive role of SO_4^{2-} groups that address the deposition of Au in the form of highly dispersed non-metallic gold clusters in close contact with the support.

References

[1] A. Corma, H. Garcia, Chem. Soc. Rev. 37 (2008) 2096–2126.
[2] R. Meyer, C. Lemire, Sh.K. Shaikhutdinov, H.-J. Freund, Gold Bull. 37 (2004) 72–124.
[3] M. Turner, V.B. Golovko, O.P.H. Vaughan, P. Abdulkin, A. Berenguer-Murcia, M.S. Tikhov, B.F.G. Johnson, R.M. Lambert, Nature 454 (2008) 981–983.
[4] D. Tibiletti, A. Amieiro-Fonseca, R. Burch, Y. Chen, J.M. Fisher, A. Goguet, C. Hardacre, P. Hu, D. Thompsett, J. Phys. Chem. B 109 (2005) 22553–22559.
[5] M. Ojeda, E. Iglesia, Angew. Chem. Int. Ed. 48 (2009) 4800–4803.
[6] F. Menegazzo, F. Pinna, M. Signoretto, V. Trevisan, F. Boccuzzi, A. Chiorino, M. Manzoli, ChemSusChem 1 (2008) 320–326.
[7] F. Menegazzo, F. Pinna, M. Signoretto, V. Trevisan, F. Boccuzzi, A. Chiorino, M. Manzoli, Appl. Catal. A 356 (2009) 31–35.
[8] X. Song, A. Sayari, Catal. Rev. Sci. Eng. 38 (1996) 329–412.
[9] V. Idakiev, T. Tabakova, A. Naydenov, Z.-Y. Yuan, B.-L. Su, Appl. Catal. B 63 (2006) 178–186.
[10] A. Kuperman, M. Moir, WO 2005-005032 (2005).
[11] M. Boaro, M. Vicario, J. Llorca, C. de Leitenburg, G. Dolcetti, A. Trovarelli, Appl. Catal. B 88 (2009) 272–282.
[12] F. Menegazzo, M. Manzoli, A. Chiorino, F. Boccuzzi, T. Tabakova, M. Signoretto, F. Pinna, N. Pernicone, J. Catal. 237 (2006) 431–434.
[13] F. Zane, V. Trevisan, F. Pinna, M. Signoretto, F. Menegazzo, Appl. Catal. B 89 (2009) 303–308.
[14] C. Sarzanini, G. Sacchero, F. Pinna, M. Signoretto, G. Cerrato, C. Morterra, J. Mater. Chem. 5 (1995) 353–360.
[15] S. Brunauer, P.H. Emmett, E. Teller, J. Am. Chem. Soc. 60 (1938) 309–319.
[16] E.P. Barrett, L.S. Joyner, P.P. Halenda, J. Am. Chem. Soc. 73 (1951) 373–380.
[17] C. Morterra, G. Cerrato, M. Signoretto, Catal. Lett. 41 (1996) 101–109.
[18] M. Signoretto, F. Pinna, G. Strukul, P. Chies, G. Cerrato, S. Di Ciero, C. Morterra, J. Catal. 167 (1997) 522–532.
[19] F. Zane, S. Melada, M. Signoretto, F. Pinna, Appl. Catal. A 299 (2006) 137–144.
[20] R. Srinivasan, R.A. Kheog, D.R. Milburn, B.H. Devis, J. Catal. 153 (1995) 123–130.
[21] B.H. Davis, R.A. Keogh, R. Srinivasan, Catal. Today 20 (1994) 219–256.
[22] S. Ardizzone, C. Bianchi, E. Grassi, Colloids Surf. 135 (1998) 41–51.
[23] C. Morterra, G. Cerrato, F. Pinna, M. Signoretto, J. Catal. 157 (1995) 109–123.
[24] E.J. Hollstein, J.T. Wei, C.Y. Hsu, US Patent 4,918,041 (1990).
[25] F. Moreau, G.C. Bond, A.O. Taylor, J. Catal. 231 (2005) 105–114.